Joint Centre for Mesoscale Meteorology, Reading, UK

Gravity wave in sheared ducts

A. J. Thorpe
S. Monserrat

Internal Report No. 18

October 1993

Met Office Joint Centre for Mesoscale Meteorology Department of Meteorology
University of Reading PO Box 243 Reading RG6 6BB United Kingdom
Tel: +44 (0)118 931 8425 Fax: +44 (0)118 931 8791
www.metoffice.com

Gravity waves in sheared ducts

S. Monserrat[1] and A.J. Thorpe[2]

[1] Dept. de Física, Universitat Illes Balears,
E-07071 Palma de Mallorca, SPAIN.

[2] Dept. of Meteorology, University of Reading,
2 Earley Gate, Whiteknights, Reading RG6 2AU, U.K.

October 13, 1993

Abstract

This paper attempts to explain the properties of a gravity wave event observed on Mallorca (Balearic Islands) using an array of microbarographs. The waves propagated coherently for a relatively long distance with a speed of about 29 m/s without any clear presence of a continuous forcing and were non-dispersive. A general matrix method to find the properties of unstable and neutral modes associated with observed atmospheric profiles is introduced. The method is first tested with some idealized cases and afterwards used on the observed profile. The role of shear in the wind profile near the ground is examined and three distinct neutral mode types are found. In the absence of a continuous forcing, long-lived atmospheric gravity waves can only exist if some mechanism prevents the vertical leakage of energy through wave propagation, trapping the gravity wave in a duct layer near the surface. Lindzen and Tung (1976) showed the necessary conditions for trapping and discussed the properties of 'almost-free' waves for constant stability and wind in the duct. Here the free neutral modes of the layer are first computed. Those free neutral modes in the sheared duct which have critical levels within the stable duct will, applying the wave theory given by Booker and Bretherton (1967), be absorbed at their critical level. Therefore they will not be observed in surface pressure measurements. On the other hand neutral modes with a critical level above the top of the duct will be reflected and so will constitute the main signal in the surface observations. This appears to explain the observations in Mallorca.

1 Introduction

In recent years, numerous papers have been addressed towards the understanding of the source mechanisms and propagation of gravity waves in the lower atmosphere. Different studies suggest gravity waves can be generated by either flow over mountains, convection, Kelvin-Helmholtz instability, or geostrophic adjustment (see, for example Gossard and Hooke 1975 or Einaudi 1980). Non-linear wave-wave interaction, suggested by some authors (Fritts 1982, 1984) can only modify the wave spectrum and cannot be considered as a source of wave activity itself.

A forcing mechanism is, of course, necessary to trigger gravity waves but, on some occasions, remarkable large amplitude atmospheric disturbances

have been recorded in regions where a continuous forcing is not observed, or far away from the suggested source region. On these occasions, whatever the energy source for these waves may be, long-lived gravity waves can only exist if some mechanism is able to trap the wave energy near the surface throughout wave propagation. Otherwise they would lose their energy through vertical propagation, normally before traveling a complete wavelength in the horizontal.

In summer 1990 some gravity wave events were detected on the Balearic Islands (western Mediterranean) by measuring surface pressure with a triangular array of microbarographs (Monserrat and Thorpe 1992). The waves were registered far away from any significant orography which might be considered responsible for the wave generation and no convection was normally reported. On the other hand, the gravity waves were observed to be long-lived, traveling long distances without significant loss of coherence. The presence of some mechanism trapping the energy near the surface must have occurred in order to explain the good correlations observed.

Lindzen and Tung (1976), hereafter referred to as LT, provided one of the most complete works on gravity wave trapping. They show the necessary conditions for the existence of an efficient wave-duct from which little wave energy leaks. The duct must be a stable layer adjacent to the surface, deep enough to maintain at least a quarter of the vertical wavelength of the ducted mode, and capped by a good reflector. An unstable layer, where the Richardson number is less than 0.25, containing a critical level optimizes the reflection. This latter layer above the wave duct would reflect the wave energy and would allow the wave propagation for several waves cycles without significant loss of energy.

Vertical profiles of the atmosphere observed on the Balearic Islands at the time of the gravity wave events exhibit a level at about 4 km where the wave trapping condition given by LT is satisfied. This indicates the possible presence of a wave duct trapping the energy at lower levels. The LT results are based on a model of 'almost free' waves with constant wind and Brunt-Väisälä frequency in the duct. Such waves exist assuming a wave source at the ground and so do not satisfy the zero vertical velocity condition at the ground. Radiosonde ascents made from the Balearic Islands clearly show that wind increases with height in the stable layer near the ground. Here the role of these variable atmospheric profiles on free modes is described. We use the trapping conditions given by LT to suggest which of these modes will be

trapped and so be observed at the ground. This constitutes the main aim of this paper.

In general, if we assume wave solutions of the form $W = W(z)e^{ik(x-ct)}$, where W is a scaled vertical velocity, k the horizontal wavenumber, the x-axis is in the direction of the wave phase propagation, and c the phase speed, the perturbation two-dimensional governing gravity wave equations can be reduced to a single equation for W with the form

$$\left(\frac{d^2}{dz^2} + \lambda^2(z)\right) W(z) = 0 \tag{1}$$

known as the Taylor-Goldstein equation (Goldstein 1931, Taylor 1931).

Any study of the stability or propagation of gravity waves in the atmosphere is based on computing the eigenvalues c and eigenfunctions W satisfying equation (1) fulfilling some given boundary conditions at the top and the bottom of the domain. Complex eigenvalues are related to unstable modes and real ones to neutral modes. In general $\lambda(z)$ is a function of the vertical profiles of wind and Brunt-Väisälä frequency and of the wavenumber and phase speed. It takes on different forms depending on the approximations assumed in the model. On some occasions, when $\lambda(z)$ has a simple form, it is possible to solve the equation analytically. However, in realistic situations $\lambda(z)$ is commonly a complicated function of z and (1) must be solved numerically.

Lalas and Einaudi (1976) used a method for obtaining the eigenvalues and eigenfunctions of the Taylor-Goldstein equation and presented the results for an hyperbolic-tangent wind profile with constant Brunt-Väisälä frequency. Later this method, with some modifications, has been used to analyse actual radiosonde ascents (Lalas and Einaudi 1980, Mobbs and Darby 1989). The method, which has been referred to as 'the shooting method', is applicable to both neutral and unstable modes, and basically consists of solving equation (1) by successive iterations, beginning with a first guess for the eigenvalue c. The major problem associated with this method is the presence of critical levels where the phase speed of the wave is equal to the wind speed. Some technique is necessary to deal with such levels as some terms in $\lambda(z)$ tend to infinity and Eq. (1) is not applicable. Another problem is the sometimes observed tendency of the method to converge to one particular mode and other modes are never found. If the first guess is far from the real solution

the model may not converge or does it very slowly. In any case, the necessity of this first guess clearly introduces an unavoidable bias in the final results. Different techniques have been used in order to minimize these problems and the method has been successfully used on many occasions, particularly for stability analysis.

Another method for solving the Taylor-Goldstein equation, which has been used much less in the literature is the so-called 'matrix method'. The method consists in reducing the solution of the Taylor-Goldstein equation to finding the eigenvalues and eigenfunctions of a given matrix. The method is more expensive in computer time but it has the advantage of not requiring a first guess, avoiding any biased result, and no special technique is necessary to deal with the critical levels. This method is then very useful when seeking neutral modes.

In this paper we solve the Taylor-Goldstein equation using the matrix method. In particular we study the influence of the wind shear on neutral free modes. The results are used to explain the properties of the gravity waves observed on the Balearic Islands in summer 1990. In section 2 the matrix method to find free modes is described and then in section 3 the method is used to reproduce some results associated with simple idealized profiles. In particular results are obtained when constant wind shear in the duct is present. Then in section 4 an attempt is made to relate the modes found with those observed in Mallorca: an interpretation in terms of wave reflection and absorption is given. In section 5 the method is used to obtain the neutral modes of a real radiosonde ascent made in the Balearic Islands during an episode of gravity waves in summer 1990. Evidence that the observed gravity waves were neutral modes trapped in a duct is given by invoking the trapping conditions suggested by LT. The results obtained with this model are in very good agreement with the observations giving an explanation for the non dispersive nature of the waves. Finally in section 6 a summary of the main results and the conclusions are presented.

2 The matrix method

The matrix method assumes the atmosphere to be built up from M layers of depth h within which the parameters are considered to be constant. We can then express U and N^2 as vectors of M components, each component

being the value of U and N^2 at this layer, assumed constant. Similarly, the function $W(z)$ is also a vector of M components

$$U(z) \rightarrow \vec{U} = (U_1, U_2, \cdots, U_M) \tag{2}$$
$$N^2(z) \rightarrow \vec{N^2} = (N_1^2, N_2^2, \cdots, N_M^2) \tag{3}$$
$$W(z) \rightarrow \vec{W} = (W_1, W_2, \cdots, W_M) \tag{4}$$

On the other hand the second derivative can be approximated by the expression

$$\frac{d^2W(z)}{dz^2} \rightarrow \frac{W_{i+1} + W_{i-1} - 2W_i}{h^2} \tag{5}$$

In general, $\lambda(z)$ in Eq. 1 is a complicated function of c, k, $U(z)$ and $N^2(z)$, however in order to simplify the algebra in describing the method, a simple version of λ is here assumed

$$\lambda^2(z) = \frac{N^2}{(U-c)^2} - k^2$$

valid when neglecting compressible terms and those involving the second derivative of U.

On this basis, Eq. (1) can be rewritten in the form

$$\left\{c^2[\frac{d^2}{dz^2} - k^2] + c[-2U(\frac{d^2}{dz^2} - k^2)] + [U^2(\frac{d^2}{dz^2} - k^2) + N^2]\right\} W = 0, \tag{6}$$

or, by using (2)-(5)

$$\left\{c^2\mathcal{A} - c\mathcal{B} - \mathcal{D}\right\} \vec{W} = 0 \tag{7}$$

where $\mathcal{A}$, $\mathcal{B}$ and $\mathcal{D}$ are matrices of M rows and M columns which, with the boundary conditions $W_0 = 0$ and $W_{M+1} = 0$, would have the form

$$\mathcal{A} = \mathcal{M} \tag{8}$$
$$\mathcal{B} = 2\vec{U}\mathcal{M} \tag{9}$$
$$\mathcal{D} = -\vec{U^2}\mathcal{M} - \vec{N^2}\mathcal{I} \tag{10}$$

where $\mathcal{I}$ is the identity matrix and $\mathcal{M}$ is a tridiagonal matrix

$$\mathcal{M} = \left(\frac{d^2}{dz^2} - k^2\right)$$

$$= \frac{1}{h^2}\begin{pmatrix} -2-k^2h^2 & 1 & 0 & 0 & 0 & \cdots \\ 1 & -2-k^2h^2 & 1 & 0 & 0 & \cdots \\ 0 & 1 & -2-k^2h^2 & 1 & 0 & \cdots \\ 0 & 0 & 1 & \ddots & 1 & \ddots \\ 0 & 0 & 0 & 1 & \ddots & \ddots \\ \vdots & \vdots & \vdots & \ddots & \ddots & \ddots \end{pmatrix} \tag{11}$$

(12)

Defining now a new vector

$$\vec{W}_1 = c\vec{W} \tag{13}$$

Equation (7) becomes

$$\mathcal{A}^{-1}\mathcal{D}\vec{W} + \mathcal{A}^{-1}\mathcal{B}\vec{W}_1 = c\vec{W}_1 \tag{14}$$

and using the definition of $\vec{W}_1$ (12), and (13) we can write

$$\begin{pmatrix} 0 & 1 \\ \mathcal{A}^{-1}\mathcal{D} & \mathcal{A}^{-1}\mathcal{B} \end{pmatrix} \begin{pmatrix} \vec{W} \\ \vec{W}_1 \end{pmatrix} = c \begin{pmatrix} \vec{W} \\ \vec{W}_1 \end{pmatrix} \tag{15}$$

or

$$\mathcal{H}\vec{\psi} = c\vec{\psi} \tag{16}$$

Here $\vec{\psi}$ is a $2M$ components vector where the first M values are the components of $\vec{W}$ and the second M values are the components of $\vec{W}_1$. Matrix $\mathcal{H}$ is a matrix with $2M$ rows and $2M$ columns including all the information about the vertical structure of the atmosphere.

The solutions of the Taylor-Goldstein equation are the eigenvalues and eigenvectors of this specified matrix $\mathcal{H}$. Equation (15) can be solved by using any commercial subroutine available. The results shown in this work

has been obtained by using a subroutine from the NAG-library. The output of the method is a set of M eigenvalues and eigenfunctions of the problem. Criteria to select some of these modes are then necessary and we will discuss these in more detail in the following sections.

For simplicity, in this section a simple form for λ has been used, however no restrictions on λ are really imposed by the method and in the following sections, the model is applied using the fully compressible version of λ. The complete form of the matrices used can be found in Appendix A.

It should be noted that for a given vertical resolution M, there will be M modes. Some of these will be of a purely numerical origin and to find the true solutions one needs to compare results for several values of M to be able to discard these non-physical solutions. As well as having the advantage of not requiring an initial guess the method also requires no special treatment in the vicinity of critical levels.

3 Free modes in stable duct profiles

The method introduced in section 3, but with the fully compressible version of $\lambda(z)$, has been tested when applied to some idealized profiles. The performance is very good when obtaining unstable modes. In particular, the results obtained with the matrix method have been compared with the shooting method results for some idealized profiles presented by Mobbs and Darby (1989). Both eigenvalues and eigenfunctions found with the two methods are identical and they are not shown here.

In this section other idealised profiles are used to determine the characteristics of the neutral and growing modes in a layer near the ground. Research to which this is related is Lindzen and Rosenthal (1976) (LR hereafter) and Monserrat and Ramis (1990). Instead of attempting to describe the complete parameter space of the dependence of the growth rate and phase speed as a function of the determining non-dimensional parameters describing the profile we set typical dimensional values suggested from the observations from Mallorca. Here we concentrate on the horizontal wavenumber dependence of the growth rates and phase speeds with special attention to the neutral modes and the dispersive nature of the waves. This will be compared with and without shear in the layer near the ground.

The results shown throughout the paper have been obtained using $M =$

100 and selecting the top of the model at a height of 6000 m implying a resolution of 60 m. When the top of the model is selected at a higher level or the value of M is increased, the results obtained are very similar. We apply the method to the case of a constant wind in a layer with $R_i = \infty$ (the lower layer) capped by a dynamically unstable (intermediate) layer where the $R_i < 0.25$ above which the wind returns to being constant with height (the upper layer) (Fig. 1a). A further analysis is to use the same profiles except that the wind in the lower layer has constant shear (Fig. 1b). This will allow the simplest description of the modification of the results due to shear in the duct.

The profile in Fig. 1a is similar to the one used by LR although there the depth of the intermediate layer is set to zero and the vertical velocity is not forced to be zero at the upper boundary. It also can be compared with that used in Monserrat and Ramis (1990) but now no discontinuity in the wind profile is considered and the Brunt-Väisälä frequency is not set to zero in the intermediate sheared layer.

We first apply the method to find the unstable modes that the profile in Fig. 1a can support. The wind (U) in this profile is symmetric about a mean value of $U_0 = 27.5\ m/s$ in the middle of the intermediate layer. To describe the modes it is useful to refer the results to this value. A number of unstable modes selected by their phase speed are found. The phase speeds of the unstable modes range between 25 m/s and 30 m/s: the minimum and maximum wind speed for this profile. This is consistent with Miles-Howard semicircle theorem (Howard 1961) which restricts the phase speed relative to the mean wind $(c - U_0)$ for unstable solutions to a semicircle of radius δU where $\delta U = U - U_0$. We can divide the unstable modes into two types, one with phase speeds greater than U_0 and the other with phase speeds less than U_0. For each mode with phase speed $c_1 < U_0$, another mode with phase speed $c_2 = U_0 + c_1$ and the same growth rate is found. Only the first type was found by LR. The second type appears as a consequence of having a rigid upper boundary. In Fig. 2 the growth rate and the phase speed for the two most unstable pairs of modes are shown. The differences observed in the growth rate curve for each pair of modes become smaller when using a larger M however, we keep these results here in order to use a single M for all calculations throughout the paper.

The neutral modes can be divided into two basic categories: modes with significant pressure response at surface and modes located at higher levels

without any such response near the ground. We are particularly interested in the former so no more comments will be made on the latter. So as to compare the different modes we give the maximum vertical velocity an arbitrary magnitude of unity. The results for neutral modes with significant response at the surface have a resemblance with those shown in Fig. 3 from LR. These are the only modes found by LR. The reason why other modes are found here can be attributed to the presence of the upper boundary and the thickness of the intermediate layer. Lindzen and Rosenthal (1976) analytically found an infinite number of neutral modes ($m = 1, 2, 3, ...$) each having $m/2$ vertical wavelengths in the lower layer. For each mode number, two types of solutions were found, one with $-U < c < 0$ and the other with $c < -U$ when the wind in the lower and the upper layer was assumed to be $-U$ and U, respectively. A similar result is reproduced here: two modes with half vertical wavelength in the lower layer ($m = 1$ in LR), one with $c < 25\ m/s$ and the other with $c > 25\ m/s$, together with a number of other higher order modes are found. The phase speeds of the '$m = 1$ modes' are the smallest and the largest phase speed the profiles can support and this range of allowed phase speeds decreases when the wavenumber increases. In Fig. 3a the normalized vertical velocity of three of these neutral modes for $k = 0.002m^{-1}(\lambda = 3km)$, are plotted versus height. The phase speed of the two '$m = 1$ modes' are for this case, $c_{min} = 21.3\ m/s$ and $c_{max} = 28.7\ m/s$; only the mode with speed $c_{min} = 21.3\ m/s$ is shown in Fig. 3a. In Fig. 3b the normalized vertical velocity for these modes but now for $k = 0.00005m^{-1}(\lambda = 125km)$ are shown. The vertical structure of the modes is similar but the range of allowed phase speeds is greater than for the case in Fig. 3a, now $c_{min} = 16.8\ m/s$ and $c_{max} = 32.4\ m/s$.

Another result, already pointed out by LR, is that higher order modes are non dispersive, and also, for large enough k the phase speeds of all the modes are essentially independent of k. The value of the wavenumber at which the phase speed noticeable changes with k depends on the parameters in the model (i.e. wind and Brunt-Väisälä frequency) so, from a practical point of view, the observed waves would appear to be essentially non-dispersive if one of the higher order modes dominates or if the observable wavelengths are small enough to be in the non-dispersive region even when no mode is dominant.

No other comments about how these modes are modified with other values of wind and Brunt-Väisälä frequency are made here. On the other hand one

of the aims of this work is to show how the presence of wind shear in the lower layer can modify these results.

First we look at the unstable modes for the profiles in Fig. 1b, to be compared with the results found with constant wind in the lower layer. The results are similar to those found without shear in the lower layer, although now the growth rates are larger and the most unstable wavelengths are shorter. Also the phase speeds of the unstable modes range between 0 m/s and 30 m/s although small phase speeds are associated with small growth rates. Five unstable modes, including the most unstable mode the profile in Fig. 1b can support ($\lambda = 722\ m, c = 25.37\ m/s$) are shown in Fig. 4.

On the other hand, the profile in Fig. 1b can support a number of neutral modes which have a clearly different behaviour to those found with constant wind in the lower layer. We can divide these modes into three different types:

- type A, located at higher levels without a significant response near the ground.
- type B, with phase speeds less than the wind speed at the top of the lower layer but greater than that at the ground: in other words these waves have a critical level in the lower layer.
- type C have a phase speed equal to the wind speed in the intermediate layer: these waves have a critical level somewhere in the intermediate layer.

Examples of the vertical structure of these 3 modes for $k = 0.0008m^{-1}$ ($\lambda = 7.85km$) are given in Fig. 5.

Type B modes have a response restricted between the ground and the critical level. This kind of mode did not appear when constant wind was assumed in the lower layer. Another difference is that now a full range of phase speeds between the surface wind and the wind speed in the upper layer is found. This means that a non dispersive nature of the observed waves cannot be explained in terms of having a short range of allowed phase speeds as before. So when wind shear is present in the lower layer, a broad range of phase speeds is in principle allowed for any k, and the waves would be non-dispersive only if some mechanism causes waves with certain phase speeds to dominate.

4 Interpretation of modes in terms of wave trapping

In the case of the sheared lower layer we have found modes which fall into the 3 categories described above as A, B, and C. It appears, from the observational evidence from the Mallorcan microbarographs, that the waves observed at the ground are essentially non-dispersive. This suggests that only some of these three types are observed at the surface. Here we attempt to give a physical explanation of this observation in terms of wave absorption and reflection as described by Booker and Bretherton (1967) and Lindzen and Tung (1976) respectively.

Lindzen and Tung (1976), analysing the necessary conditions for the presence of ducted waves in the atmosphere, basically discussed the necessary properties of an effective reflecting layer able to maintain wave energy near the surface. They showed that the presence of a critical level or at least a nearly critical level either in or above an unstable layer capping a stable duct is optimal for reflecting the waves. If we assume the reflecting layer is present, the ducted wave properties will be governed by the duct characteristics. Assuming simple atmospheric profiles for wind and Brunt-Väisälä frequency in the duct, some general comments can be made. Some of these have already been noted by LT.

In the Taylor-Goldstein equation (Eq. 1) $\lambda^2(z)$ is normally written as

$$\lambda^2(z) = \ell^2(z) - k^2 \tag{17}$$

where $\ell^2(z)$ is known as the Scorer parameter.

The vertical propagation of the gravity waves is basically controlled by $\ell^2(z)$ which can be approximated (neglecting compressible terms and the terms including the second derivative of U) by the expression

$$\ell^2(z) = \frac{N^2}{(U-c)^2} \tag{18}$$

When the Scorer parameter is larger than k^2 the vertical wavenumber is real, representing oscillatory waves, on the other hand, when it is smaller than k^2, the solutions are imaginary, the wave is evanescent, and its amplitude decays exponentially with distance away from the source height. Therefore,

an oscillatory ducted mode can only exist in a stable layer and N^2 must be large enough for the Scorer parameter to be larger than k^2.

Another important aspect related to the vertical propagation of the waves is the presence of critical levels where the Scorer parameter approaches infinity for neutral modes. The vertical velocity of neutral modes becomes zero at these levels and the energy is reflected if the layer is unstable or absorbed if it is stable (Booker and Bretherton 1967).

As LT indicate in their paper to be a ducted mode a wave should not have a critical level in the duct because if it did then wave energy would be absorbed rather than reflected. However if there is wind shear in the duct then it is clear that different modes (or different phase speeds) will have a critical level at different heights. This is likely to be important in determining the dominant mode in the duct. The dominant ducted mode was considered by LT to be the one with largest phase speed because the other ones, related to shorter vertical wavelengths, would be more significantly attenuated by any dissipative process. In a duct with constant wind shear there will be modes with phase speeds equal to the wind at some level inside the duct. These will, following the reasoning of Booker and Bretherton (1967), be absorbed at their critical level. This means that in the presence of wind shear, the duct has another mechanism aside from dissipation for selecting the dominant trapped mode.

This analysis suggests that wind shear, or any other vertical variation in λ, plays an important role in determining the expected ducted modes.

We can now summarize these conclusions for the 3 wave types found:

- type A, have no response near the ground and they are confined in some upper layer. The wave energy is expected to remain aloft and so the waves are not going to be observed at surface.

- type B, are modes confined between the surface and a critical level situated within this layer. This implies, using the Booker and Bretherton (1967) criterion, that the wave energy would be absorbed at this level and these modes are therefore expected to be short lived.

- type C have a phase speed equal to the wind speed in the intermediate layer, and so using the LT argument, these waves would be trapped between the surface and a critical level situated in a layer where ($R_i <$ 0.25). The wave energy would be reflected at this level and remain

trapped in the layer near the surface. We are expecting then that this mode is going to be the dominant one at the surface.

This means that we expect the dominant modes at the surface, for any wavelength, to be type C modes. These will have a phase speed in the range of the wind speed over the intermediate layer. If this range is not large then the waves will be observed at the surface to be essentially non-dispersive.

The type C modes for constant wind shear in the lower layer have a structure with a half wavelength in the vertical, see Fig. 5. In contrast the trapped 'almost free' modes of LT have a structure with a quarter wavelength in the vertical. This difference is clearly related to the crucial difference between free and 'almost free' modes. Of course in the case of free modes we can only surmise the trapping conditions as we do not directly describe the reflection process. Here we have taken the trapping condition from the Booker and Bretherton (1967) and LT analyses.

5 Use of the method in a case study

Time series of surface atmospheric pressure from three microbarographs situated on Mallorca (Balearic Islands) were used by Monserrat and Thorpe (1992) (MT hereafter) to obtain the horizontal properties of some traveling gravity wave events observed in summer 1990. The measured waves propagated with a phase speed of about 29 m/s and were basically non dispersive. Wavelength, phase speed and wave direction of propagation for one of the episodes presented by MT is given in figure 13 of that paper. Both phase speed and wave direction are basically independent of frequency. In this section we are going to refer mainly to this episode, the one with largest pressure oscillations, which is referred to as case 3 in MT.

The non dispersive nature of the waves is an indicator suggesting that the waves could be generated by dynamic instability. Waves generated by dynamic instability tend to travel with phase speeds and directions matching the wind speeds and directions at the level of the minimum Richardson number and they are non dispersive. MT found that, although this was not the case in every episode, in case 3, the phase speed of the wave were very similar to the wind speed at the level of minimum Richardson number, and the direction of propagation of the wave was just about 20 degrees different from the wind direction. On the other hand, although in case 3 the

Richardson number is actually zero in a layer of about 500 m, in some of the other observed cases, the Richardson number is not small enough for dynamic instability. If we consider that just one mechanism is responsible for the generation in every gravity wave episode, we cannot prove at this point that this is dynamical instability. Whatever the source mechanism the non dispersive nature of the waves has to be explained. Another point to be considered is that maybe the available soundings are more representative of the propagation region of the wave rather than of the generation region and they are not adequate to find evidence of dynamic instability.

On the other hand, good correlation between two instruments situated at a relatively long distance (more than half the measured horizontal wavelength) were observed. So, whatever the source mechanism is, the good correlations found can only be explained if the wave becomes neutral and the energy remains trapped near the surface.

The vertical profiles of wind and Brunt-Väisälä frequency fulfill the conditions suggested by LT in order to have an effective duct trapping the waves but, the idealized vertical profiles used by LT in the stable duct cannot be applied to our case. The vertical profiles of Brunt-Väisälä frequency, wind speed resolved in the measured direction of propagation of the waves (230°), and Richardson number corresponding to the radiosonde ascent made at Palma de Mallorca on 25 Sep 1992 at 0000 GMT, the closest one in time to the observation of the most energetic waves is shown in Fig. 6. It can be seen that the wind rapidly increases from calm at the surface to a maximum value of about 29 m/s at a height of about 3800 m, suggesting that assuming a constant wind profile in the stable layer near the ground may introduce spurious results. It is expected then that the presence of wind shear in the duct will introduce some modifications as discussed in the previous sections.

First we use the method to compute the unstable modes that the profile shown in Fig. 6 can support. A number of unstable modes with phase speed ranging between 0 m/s and 29 m/s are found.The most unstable mode has a phase speed of about 6 m/s and a maximum growth rate of 0.0027 s^{-1} at a wavelength of 450 m. This wavelength is too short to be observed with the array used by MT. For the range of observable wavelengths, say $4 - 200$ km, the maximum growth rate is for $\lambda = 4$ km with a maximum growth rate of 0.0004 s^{-1}, this corresponding to an e-folding time of about 45 min. Consequently for other observable wavelengths the growth rates are lower, for example the maximum growth rate for a wavelength of 15 km is

$0.0002\ s^{-1}$ (e-folding time greater than an hour). We do not really know the time scale of the processes maintaining the unstable profiles in Fig. 6, but it is perhaps unlikely than any unstable profile could be maintained for so long. Therefore we do not expect these unstable modes have much influence in the surface measurements.

We are interested in knowing if the real atmospheric profile corresponding to this case can support neutral waves with the observed phase speed and if these waves are non-dispersive. Therefore, the method introduced in section 3 is applied to the profile shown in Fig. 6 for different values of the wavenumber k corresponding to wavelengths ranging between 4 and 200 km in order to compare the results with the observations.

When the method is applied to real atmospheric profiles, for each wavenumber a number of neutral modes with different phase speeds are obtained. In Fig. 7 the modulus of the vertical velocity, related to the trapped neutral mode with the largest phase speed, is plotted versus height for two different wavelengths, 125 km and 4 km. The phase speed of the mode is also indicated in the figure. The mode is clearly confined between the surface and a layer situated at about 4000 m and hence is a type C mode. The vertical structure for both wavenumbers is somewhat different near the surface as can be expected if considering the value of the Scorer parameter. Instead of the quantity ℓ^2, the value of $\lambda_\ell = 2\pi(U-c)/N = 2\pi/\ell$ for $c = 29\ m/s$ is plotted in Fig. 8. For short wavelengths the quantity $(\ell^2 - k^2)$ becomes negative (or $\lambda_\ell > \lambda$), especially in the lowest kilometres and the wave is expected to be evanescent in this layer, as is actually found. This can be seen in Fig. 7b where the wave, with a wavelength of 4 km, has its amplitude maximized at around 3 km where $\lambda_\ell < \lambda$.

The other mode types A and B with different phase speeds are also found. Type A modes have response restricted to upper layers and then they are not expected to be relevant in surface measurements. Type B modes, with smaller phase speed, are observed to be confined in the vertical. Figure 9a shows the modulus of the vertical velocity plotted against height for $\lambda = 10\ km$ and $c = 16.5\ m/s$. We clearly see the fact pointed out in section 4: modes related with smaller phase speeds reach a critical level at a lower height. For these modes the 'top of the duct' is marked by a critical level situated in a layer where the Richardson number is greater than 0.25, with the only exception of a narrow layer situated at a height of about 1800 m. We expect then, that the wave energy is going to be absorbed rather than

reflected at this level and the mode is going to be short-lived. Some other modes, with larger phase and response in the whole domain, are also found. These waves are non-trapped and can propagate freely between the bottom and the top of the model. This can be seen in Fig. 9b, where the modulus of the vertical velocity for $\lambda = 10\ km$ and $c = 32.6\ m/s$ is plotted versus height. The presence of the upper rigid lid in the model is artificial and then we do not expect a wave trapped in the entire domain is realistic. In this case we assume the wave energy will be rapidly lost from the surface layer into the upper troposphere.

Another aspect which cannot be separated from the propagation of the waves is the height at which they are actually generated. If we assume that the waves are generated by dynamic instability, they would be generated at a height of about 4000 m, where $R_i < 0.25$. It is clear then that the energy would never reach the surface if the wave finds its critical level on its way down. When the phase speed of the mode is smaller than about $28 - 29 m/s$ (Type B modes) this is going to happen at some height between the generation height and the surface and the wave is not going to be observed at the surface.

Therefore, from the different modes that the actual atmospheric profile can support we should observe the modes which are trapped by the layer where the Richardson number is less than 0.25 which, in our case, are also the confined modes with the largest phase speed. The phase speed of these modes range between 28 m/s and 29/s and are independent of the wavenumber k (we can observe in Fig. 7 that the phase speed for the two wavenumbers is similar) and then they are clearly non-dispersive. The results suggest then, we should observe a range of wavelengths each one traveling with phase speeds around 28-29 m/s, in very good agreement with the actual observations.

We can conclude then that the observed waves in this case are probably trapped modes in a duct. The source mechanism is unclear but could be associated with dynamic instability of the wind shear as suggested by MT but cannot be confirmed without a good knowledge of the vertical structure of the atmosphere upstream.

6 Summary and conclusions

The presence of a stable layer capped above by a good reflector is the general condition for the presence of ducted waves in the lower atmosphere. Provided the existence of an efficient reflecting layer, the ducted wave properties are governed by the characteristics of the stable layer.

When constant wind and Brunt-Väisälä profiles are considered, a number of free modes can be present in the duct and their structure can be obtained solving the Taylor-Goldstein equation analytically.

Some simple arguments show that when wind shear is present in the duct, the number of modes are clearly reduced by wave absorption at critical levels. However, in general, when wind and Brunt-Väisälä frequency are functions of height, the gravity wave properties have to be found numerically.

A method able to find the neutral modes associated with given atmospheric profiles: the matrix method, is introduced and applied to the case of constant wind shear in a stable duct. The matrix method does not require any first guess and the only difficulty is reduced to select the mode of your interest from all the modes result of the given vertical profiles. The method can be applied to any real atmospheric profiles and no limitations are presented by the complexity in $\lambda(z)$. As an example, it has been used to study the waves properties in a case study on the Balearic Islands.

The model results suggest that the dominant mode associated with the vertical atmospheric profiles observed during the gravity wave episode has a phase speed similar to the measured one. Also, the non dispersive nature of the gravity wave is reproduced by the model so the dominant phase speed is essentially independent of the wavelength.

We consider the interpretation given in this paper of the non-dispersive nature of the observed waves to be speculative in the sense that we have not described the dynamics of wave absorption and reflection explicitly. Rather, results from theoretical studies of Booker and Bretherton (1967) and Lindzen and Tung (1976) have been applied to the case studied here. Research is in progress to describe these processes in a non-hydrostatic numerical model simulation. In such simulations a source of gravity waves is imposed at various levels and the horizontal (and vertical) propagation is examined. Then the hypothesis suggested herein concerning wave trapping and surface pressure fluctuations can be fully tested.

Acknowledgments. Part of this work was done during one year visit of one of us (SM) to the Dept. of Meteorology of the University of Reading under a grant from the Ministerio de Educación y Ciencia of Spain. Economical support from the project PB89-0428 of the DGICYT of Spain and the British-Spanish Joint Research Programme HB-030 is also acknowledged.

APPENDIX A

When the fully compressible version of $\lambda(z)$ is used in (1), still a matrix equation as (14) is obtained but now $\mathcal{A}$, $\mathcal{B}$ and $\mathcal{D}$ have a more complicated form.

$$\mathcal{A} = \mathcal{M} + \vec{V}_A \mathcal{I} \tag{19}$$

$$\mathcal{B} = 2\vec{U}\mathcal{M} + \vec{V}_B \mathcal{I} \tag{20}$$

$$\mathcal{D} = -\vec{U}^2 \mathcal{M} + \vec{V}_D \mathcal{I} \tag{21}$$

where $\mathcal{M}$ has the same form than in (11) and

$$\vec{V}_A = \frac{1}{4\vec{\rho}_0}\left(\frac{d\vec{\rho}_0}{dz}\right)^2 - \frac{1}{2\vec{\rho}_0}\left(\frac{d^2\vec{\rho}_0}{dz^2}\right) + \frac{\vec{N}^2}{{C_s}^2} \tag{22}$$

$$\begin{aligned}\vec{V}_B = & -\left(\frac{d^2\vec{U}}{dz^2}\right) - \frac{\vec{U}}{\vec{\rho}_0}\left[\frac{-1}{2\vec{\rho}_0}\left(\frac{d\vec{\rho}_0}{dz}\right)^2 + \left(\frac{d^2\vec{\rho}_0}{dz^2}\right)\right] \\ & -\frac{d\vec{U}}{dz}\left[\frac{1}{\vec{\rho}_0}\left(\frac{d\vec{\rho}_0}{dz}\right) + \frac{2g}{{C_s}^2}\vec{1}\right] + \frac{2\vec{U}\vec{N}^2}{{C_s}^2}\end{aligned} \tag{23}$$

$$\begin{aligned}\vec{V}_D = & -\vec{N}^2 + \vec{U}\left(\frac{d^2\vec{U}}{dz^2}\right) - \frac{\vec{U}^2}{2\vec{\rho}_0}\left[\frac{1}{2\vec{\rho}_0}\left(\frac{d\vec{\rho}_0}{dz}\right)^2 - \left(\frac{d^2\vec{\rho}_0}{dz^2}\right)\right] \\ & +\vec{U}\frac{d\vec{U}}{dz}\left[\frac{1}{\vec{\rho}_0}\left(\frac{d\vec{\rho}_0}{dz}\right) + \frac{2g}{{C_s}^2}\vec{1}\right] - \frac{\vec{U}^2\vec{N}^2}{{C_s}^2}\end{aligned} \tag{24}$$

Here, ρ_0 is the basic state density, ${C_s}^2$ the speed of sound and $\vec{1}$ the unity vector.

When compressible terms and those involving the second derivative of U are neglected, $\vec{V}_A$, $\vec{V}_B$ and $\vec{V}_D$ have the simple form given in section 2, i.e.

$$\vec{V}_A = \vec{0} \tag{25}$$

$$\vec{V}_B = \vec{0} \tag{26}$$

$$\vec{V}_D = -\vec{N}^2 \tag{27}$$

REFERENCES

Booker, J. R. and F. P. Bretherton, 1967: The critical layer for internal gravity waves in a shear flow, *J. Fluid. Mech.*, **27**, 513-539.

Einaudi, F., 1980: 'Gravity waves and the atmospheric boundary layer'. In *Atmospheric planetary boundary layer physics.* Ed. A. Longhetto. Elsevier, Amsterdam.

Fritts, D. C., 1982: Shear excitation of atmospheric gravity waves, *J. Atmos. Sci.*, **39**, 1936-1952.

Fritts, D. C., 1984: Shear excitation of atmospheric gravity waves. Part II: Non linear radiation from a free shear layer, *J. Atmos. Sci.*, **41**, 524-537.

Goldstein, S., 1931: On the stability of superposed streams of fluid of different densities. *Proc. Roy. Soc. London*, **A132**, 524-548.

Gossard, E. E. and W. H. Hooke, 1975: *Waves in the Atmosphere: Atmospheric Infrasound and Gravity Waves. Their Generation and Propagation.* Elsevier, 456pp.

Howard, L.N., 1961: Note on a paper of John W. Miles. *J. Fluid. Mech.*, **10**, 509 -512.

Lalas, D. P. and F. Einaudi, 1976: On the characteristics of gravity waves generated by atmospheric shear layers. *J. Atmos. Sci.*, **33** , 1248 -1259.

Lindzen, R. S. and A. J. Rosenthal, 1976: On the instability of Helmholtz velocity profiles in stably stratified fluids when a lower boundary is present. *J. Geophys. Res.*, **81** , 1561-1571.

Lindzen, R. S. and K. K. Tung, 1976: Banded convective activity and ducted gravity waves. *Mon. Wea. Rev.*, **104**, 1602-1617.

Mobbs, S. D. and M. S. Darby, 1989: A general method for the linear stability analysis of stratified shear flows. *Q. J. R. Meteor. Soc.* , **115**,

915-939.

Monserrat, S. and C. Ramis, 1992: Dynamic stability of a three-layer model with discontinuous profiles of wind and temperature. *J. Atmos. Sci.*, **47**, 2108-2114.

Monserrat, S. and A.J. Thorpe, 1992: Gravity wave observations using an array of microbarographs in the Balearic Islands. *Q. J. R. Meteor. Soc.* , **118**, 259-282.

Taylor, G. I., 1931: Effect of variation of density on the stability of superposed streams of fluid. *Proc. Roy. Soc. London*, **A132**, 499-523.

FIGURE CAPTIONS

Figure 1. Wind (U) and Brunt-Väisälä frequency (N) for the profiles used in section 3, with constant wind in the lower layer (a), and with constant wind shear in the lower layer (b). The name of the different layers and the value of the Richardson number in each layer are also indicated.

Figure 2. (a) Phase speed and (b) growth rate plotted against wavenumber of the four most unstable modes for the profiles in Fig. 1a. The growth rate for modes 1 and 3 and for modes 2 and 4 are almost identical.

Figure 3. The modulus of the normalized vertical velocity for three neutral modes supported by the profiles given in Fig. 1a. The wavenumber is $k = 0.002m^{-1}$ in (a), and $k = 0.00005m^{-1}$ in (b). The phase speed of the modes are indicated in the figure.

Figure 4. (a) Phase speed and (b) growth rate plotted against wavenumber of five unstable modes for the profiles in Fig. 1b. Mode 1 corresponds to the most unstable mode that this profile can support. The growth rate for mode 2 has a different behaviour, probably because it is formed by two different modes overlapped

Figure 5. The modulus of the normalized vertical velocity for the three types modes that the profiles from Fig. 1b can support. The wavenumber is $k = 0.0008m^{-1}$.

Figure 6. Wind speed resolved in the measured direction of propagation of the waves (230°) (solid line) and Brunt-Väisälä frequency (dashed line) (a) and Richardson number (b), corresponding to the radiosonde ascent made at Palma de Mallorca on 25 Sep 1992 at 0000 GMT.

Figure 7. The modulus of the normalized vertical velocity for the trapped neutral mode with the largest phase speed for $\lambda = 125km$ (a) and $\lambda = 4km$ (b). The values of the phase speed of these modes are indicated in the figure.

Figure 8. The wavelength associated with the Scorer parameter $\lambda_\ell = 2\pi(U - c)/N$ for $c = 29m/s$ corresponding to the radiosonde ascent made at Palma

de Mallorca on 25 Sep 1992 at 0000 GMT.

Figure 9. The modulus of the normalized vertical velocity for a neutral mode type B (a) and a mode non-trapped, occupying the whole domain (b) for$\lambda = 10km$. The values of the phase speed of these modes are indicated in the figure.

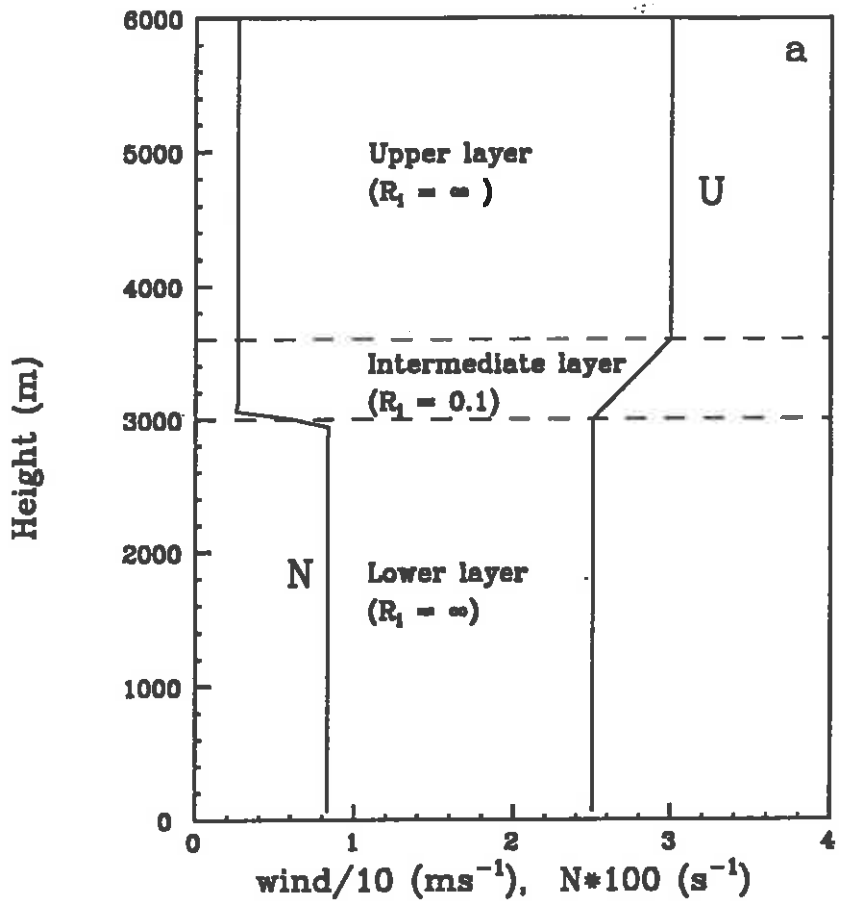
a
Upper layer
(R_i = ∞)
U
Intermediate layer
(R_i = 0.1)
N
Lower layer
(R_i = ∞)
Height (m)
6000
5000
4000
3000
2000
1000
0
0
1
2
3
4
wind/10 (ms^{-1}), N*100 (s^{-1})

Fig. 1a

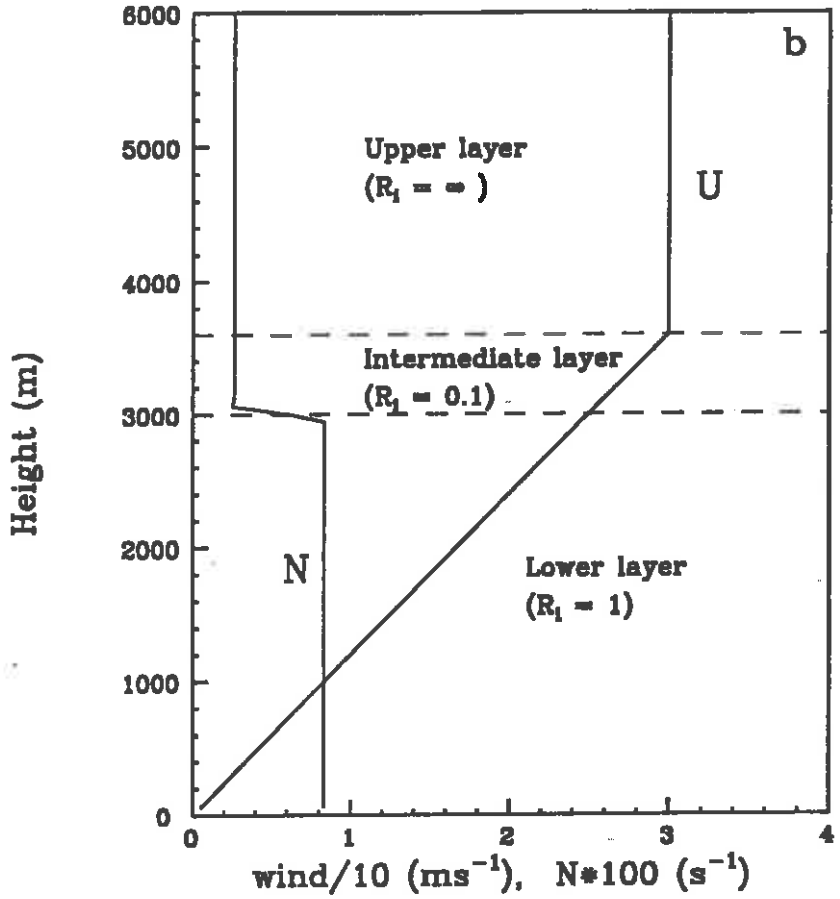
b
Upper layer
(R_i = ∞)
U
Intermediate layer
(R_i = 0.1)
N
Lower layer
(R_i = 1)
Height (m)
6000
5000
4000
3000
2000
1000
0
0
1
2
3
4
wind/10 (ms^{-1}), N*100 (s^{-1})

Fig. 1b

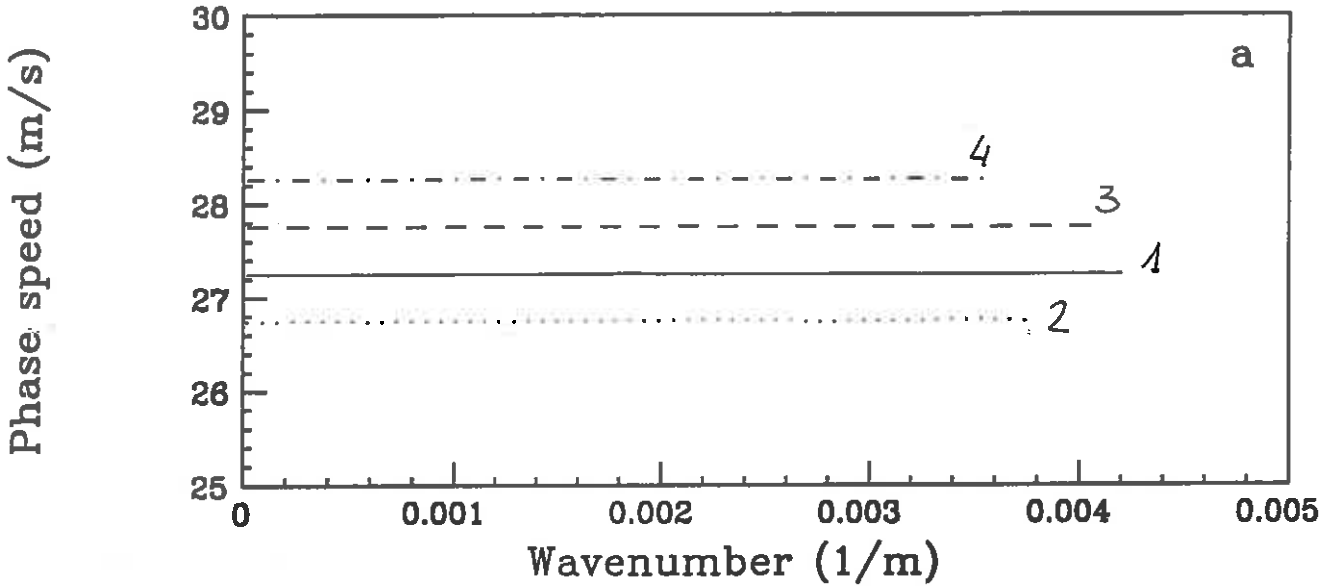
Phase speed (m/s)
30
29
28
27
26
25
0
0.001
0.002
0.003
0.004
0.005
Wavenumber (1/m)
a
4
3
1
2

Fig. 2a

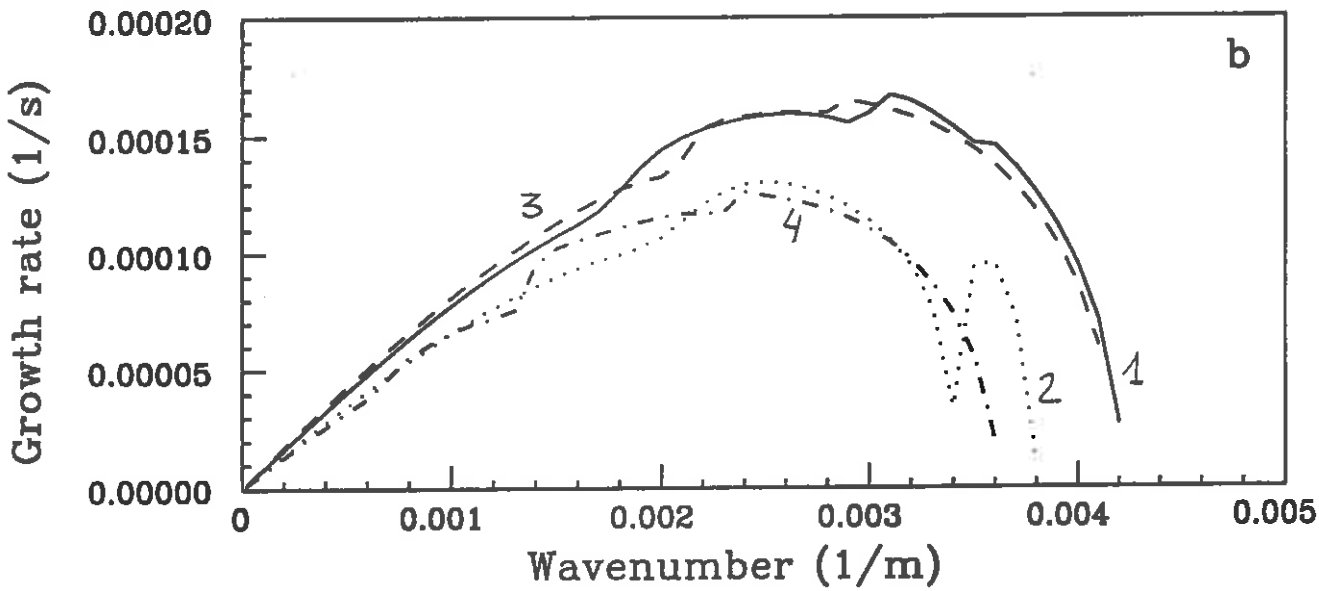
b
Growth rate (1/s)
0.00020
0.00015
0.00010
0.00005
0.00000
0
0.001
0.002
0.003
0.004
0.005
Wavenumber (1/m)
1
2
3
4

Fig. 2b

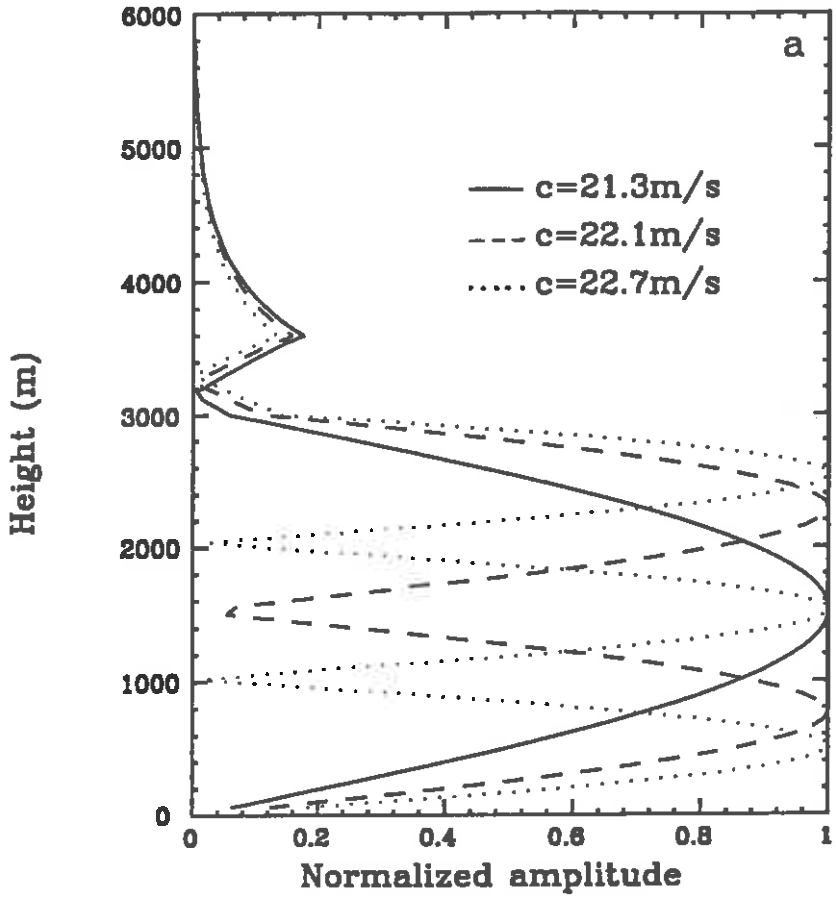
a
c=21.3m/s
c=22.1m/s
c=22.7m/s
Height (m)
Normalized amplitude
6000
5000
4000
3000
2000
1000
0
0
0.2
0.4
0.6
0.8
1

Fig. 3a

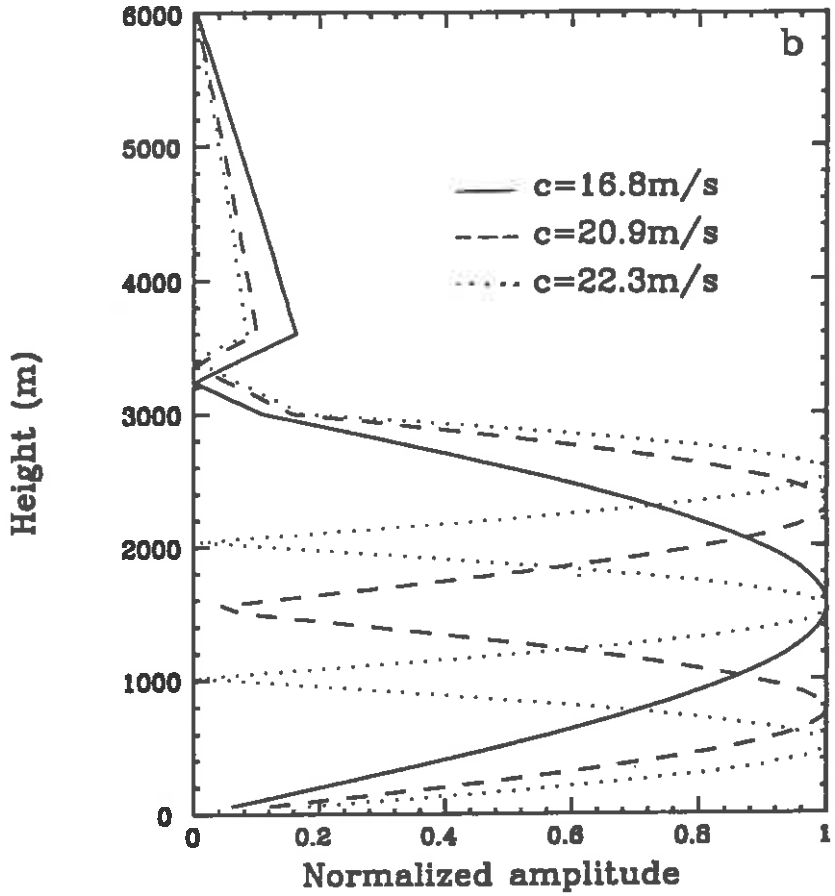
b
c=16.8m/s
c=20.9m/s
c=22.3m/s
Height (m)
6000
5000
4000
3000
2000
1000
0
0
0.2
0.4
0.6
0.8
1
Normalized amplitude

Fig. 3b

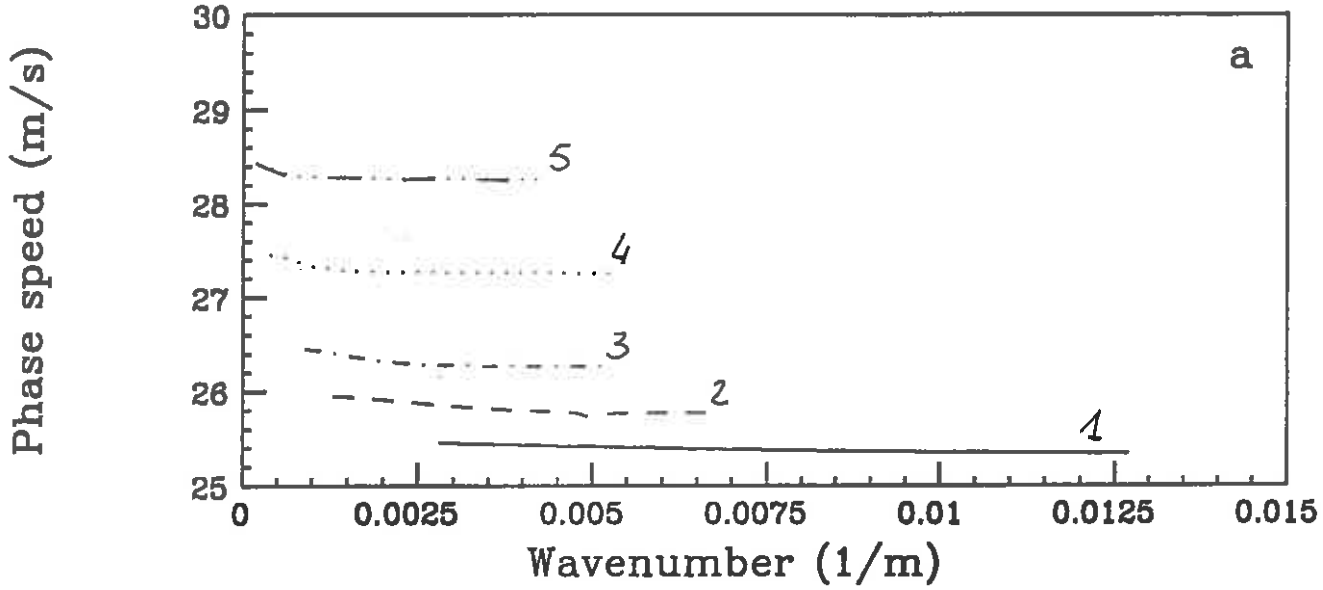
Phase speed (m/s)
30
29
28
27
26
25
a
5
4
3
2
1
0
0.0025
0.005
0.0075
0.01
0.0125
0.015
Wavenumber (1/m)

Fig. 4a

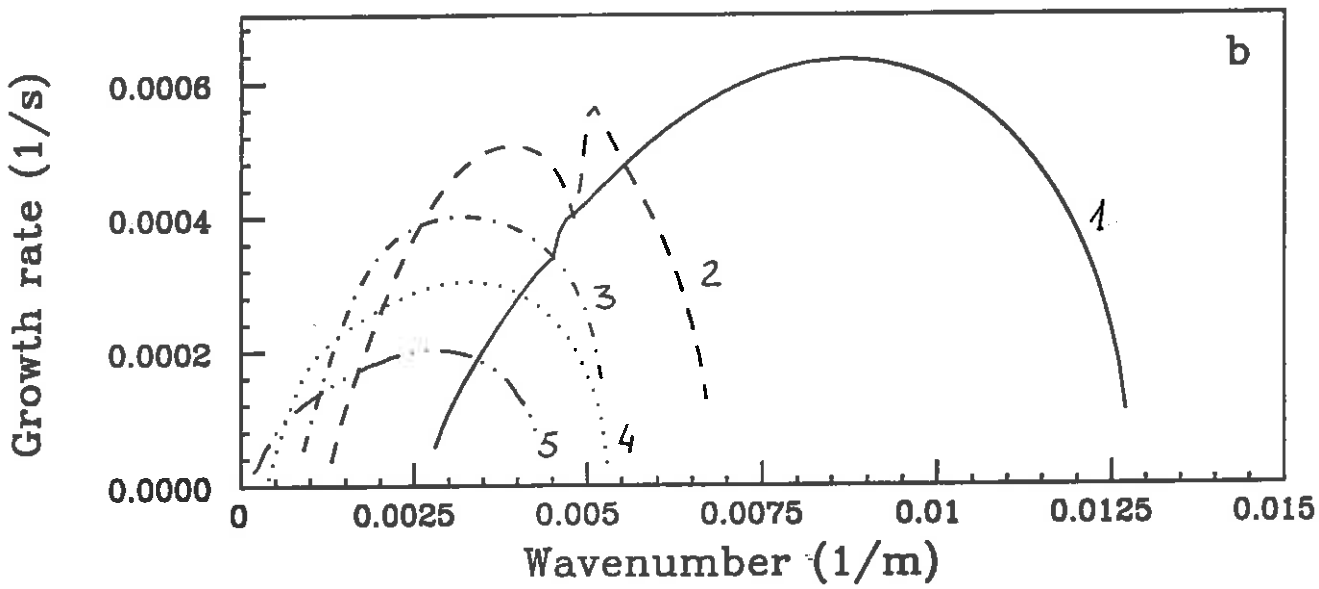
b
Growth rate (1/s)
0.0006
0.0004
0.0002
0.0000
0
0.0025
0.005
0.0075
0.01
0.0125
0.015
Wavenumber (1/m)
1
2
3
4
5

Fig. 4b

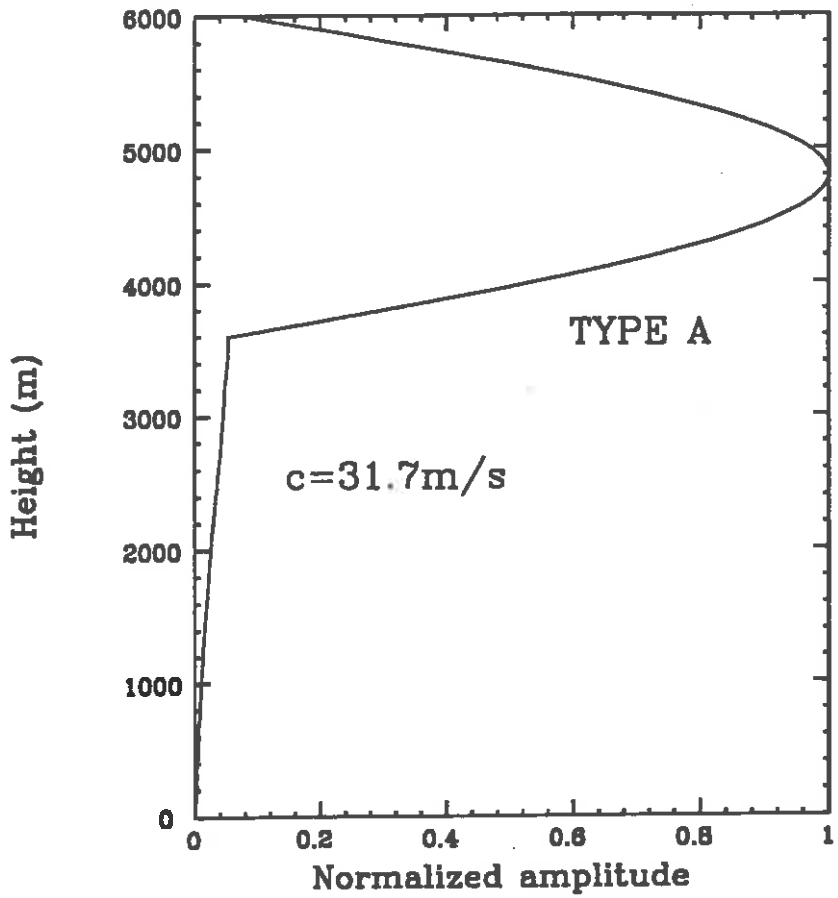
6000
5000
4000
3000
2000
1000
0
Height (m)
TYPE A
c=31.7m/s
0
0.2
0.4
0.6
0.8
1
Normalized amplitude

Fig. 5

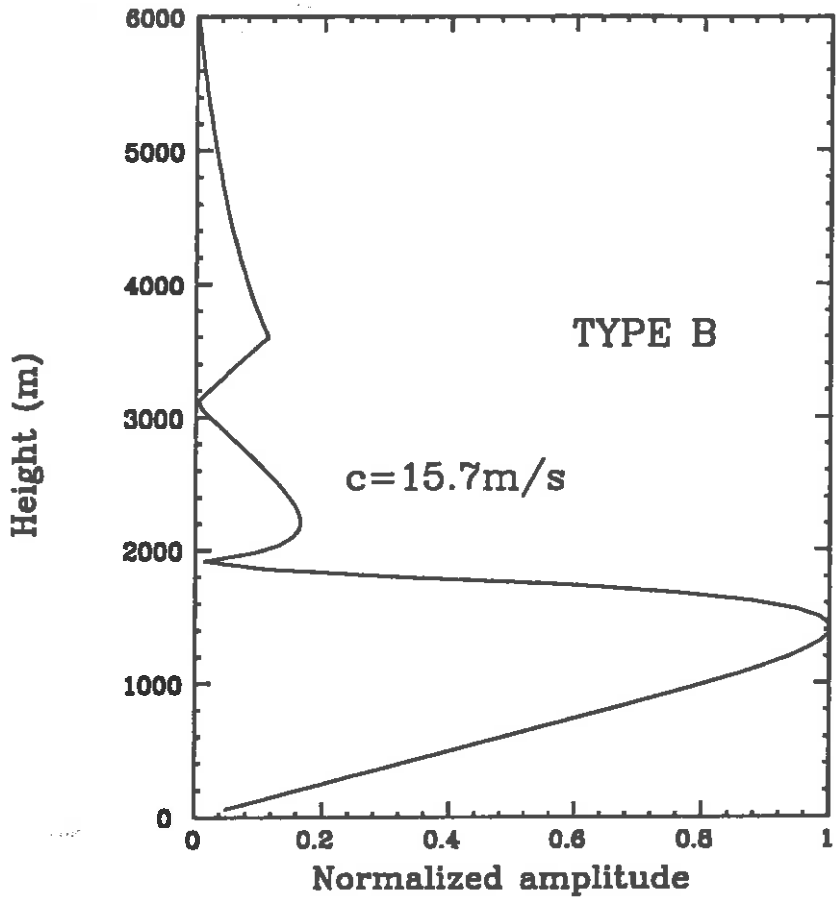
6000
5000
4000
3000
2000
1000
0
Height (m)
TYPE B
c=15.7m/s
0
0.2
0.4
0.6
0.8
1
Normalized amplitude

Fig. 5

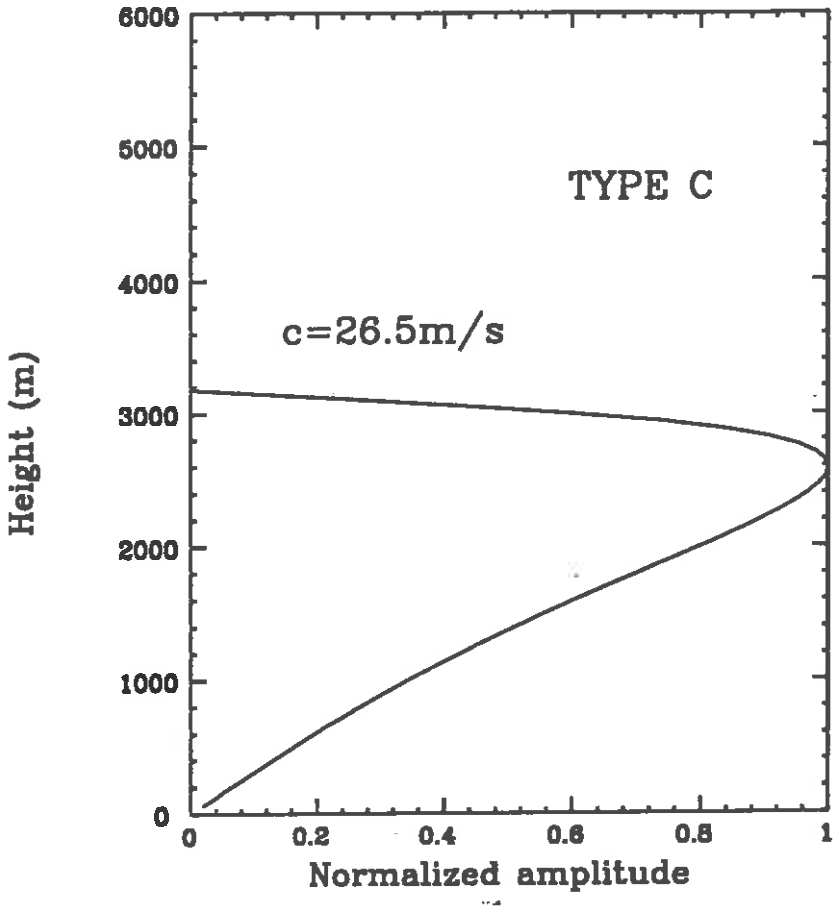
TYPE C
c=26.5m/s
Height (m)
Normalized amplitude
6000
5000
4000
3000
2000
1000
0
0
0.2
0.4
0.6
0.8
1

Fig. 5

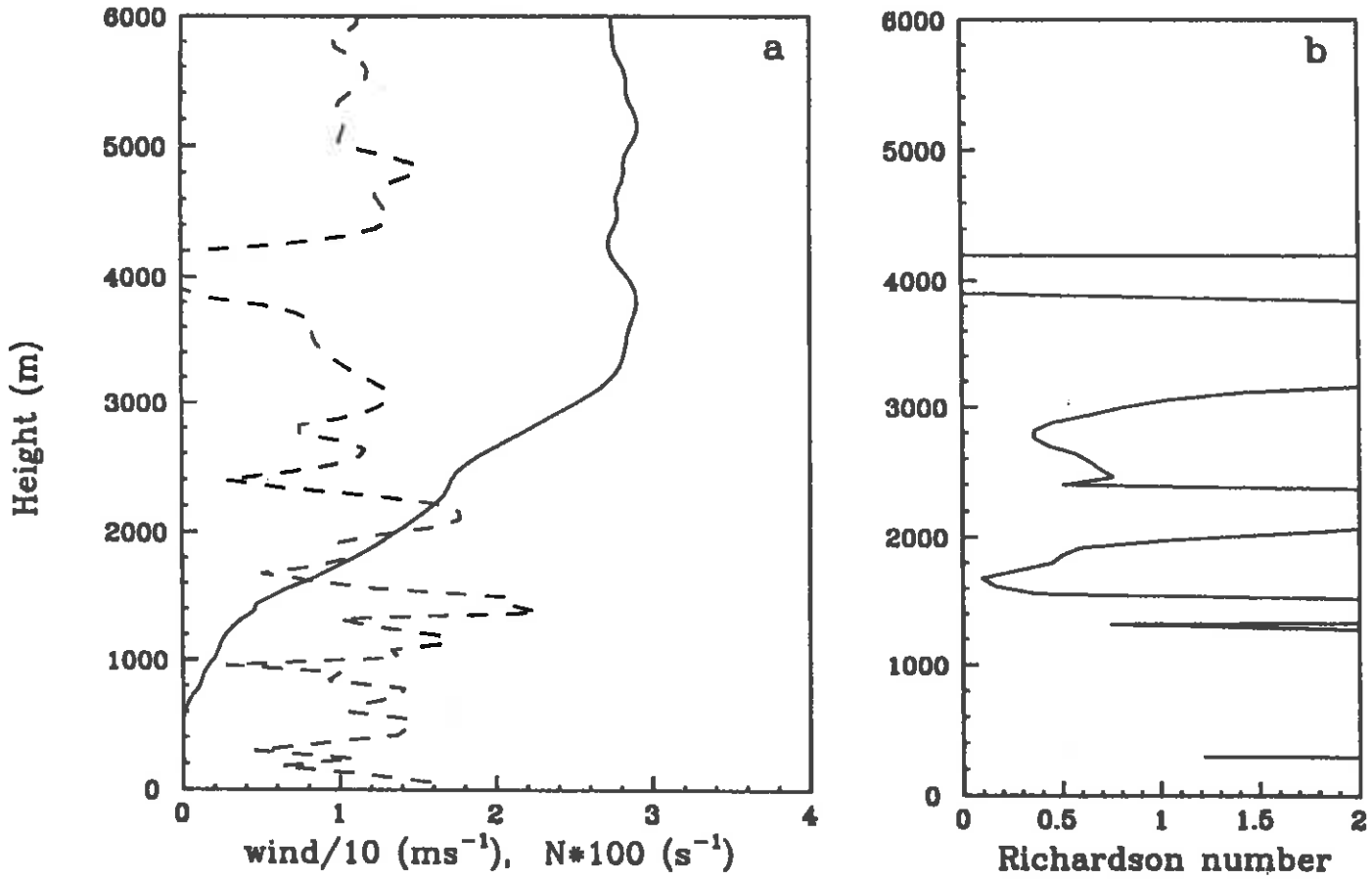
a
b
Height (m)
6000
5000
4000
3000
2000
1000
0
0
1
2
3
4
wind/10 (ms^{-1}), N*100 (s^{-1})
0
0.5
1
1.5
2
Richardson number

Fig. 6

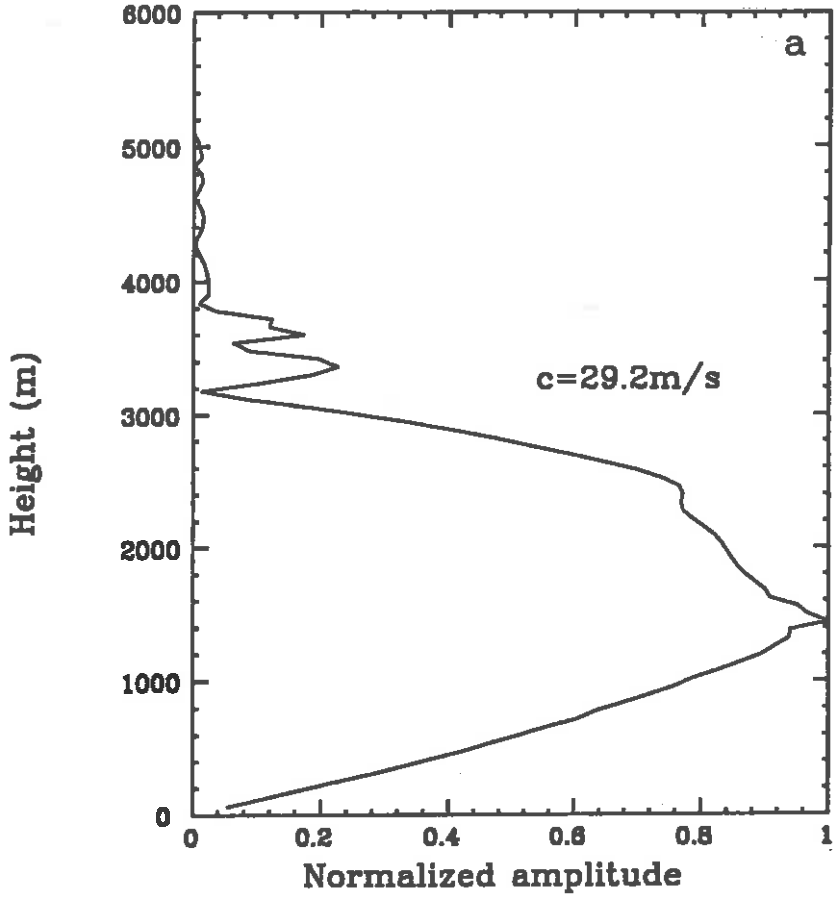
a
c=29.2m/s
Height (m)
Normalized amplitude
6000
5000
4000
3000
2000
1000
0
0
0.2
0.4
0.6
0.8
1

Fig. 7a

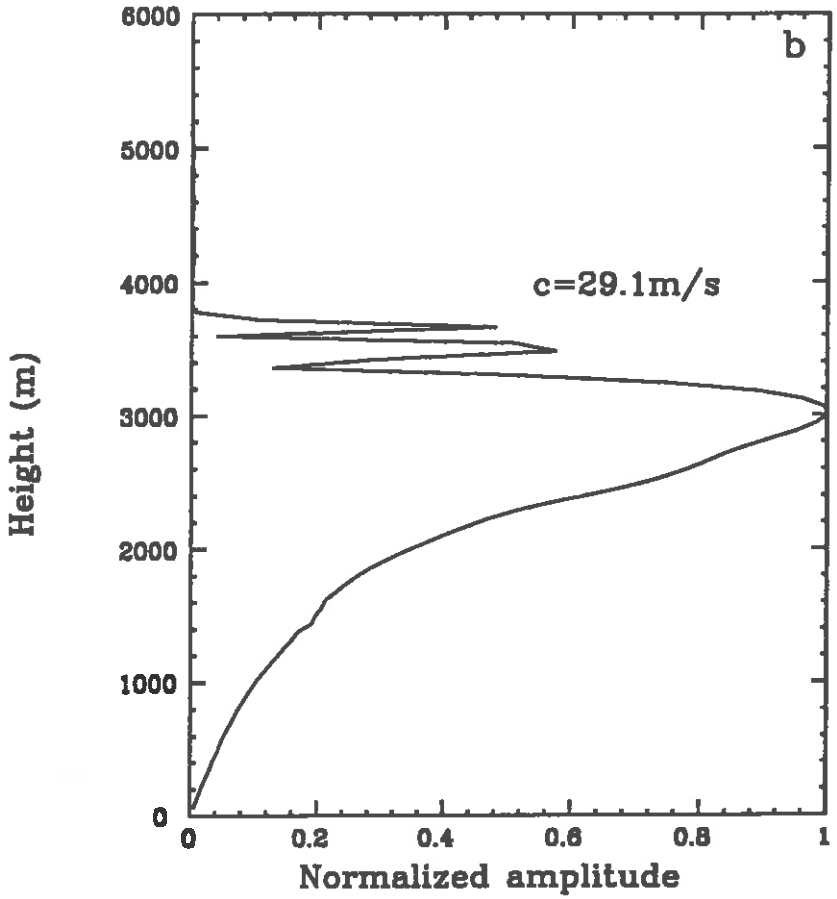
b
c=29.1m/s
Height (m)
Normalized amplitude
6000
5000
4000
3000
2000
1000
0
0
0.2
0.4
0.6
0.8
1

Fig. 7b

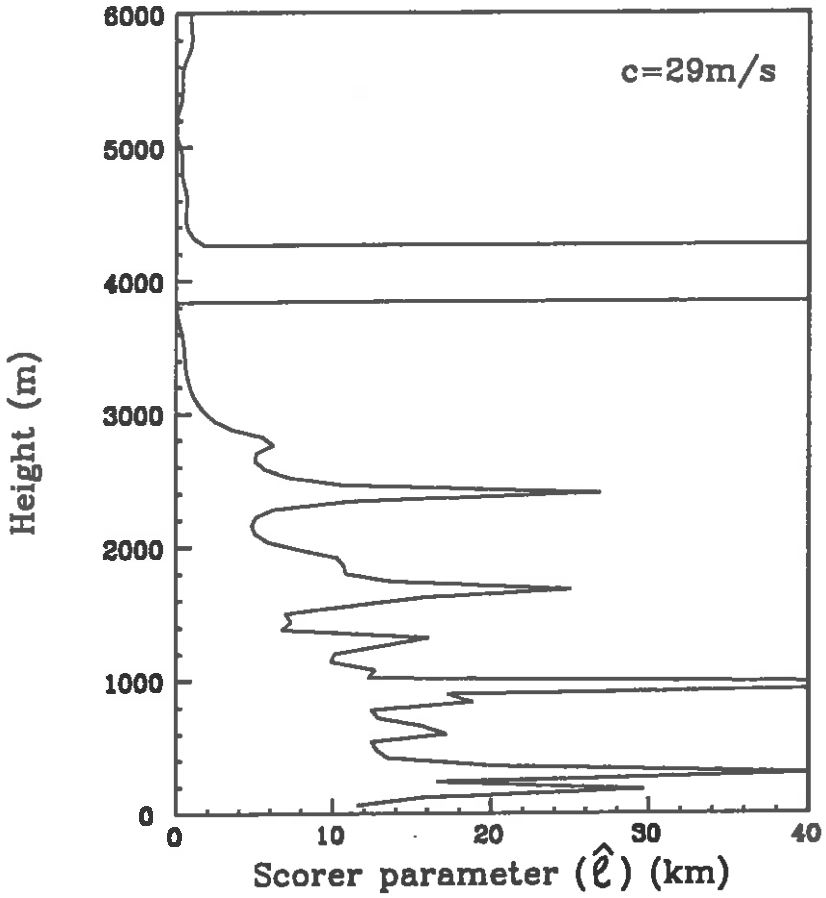
c=29m/s
Height (m)
6000
5000
4000
3000
2000
1000
0
0
10
20
30
40
Scorer parameter ($\hat{\ell}$) (km)

Fig. 8

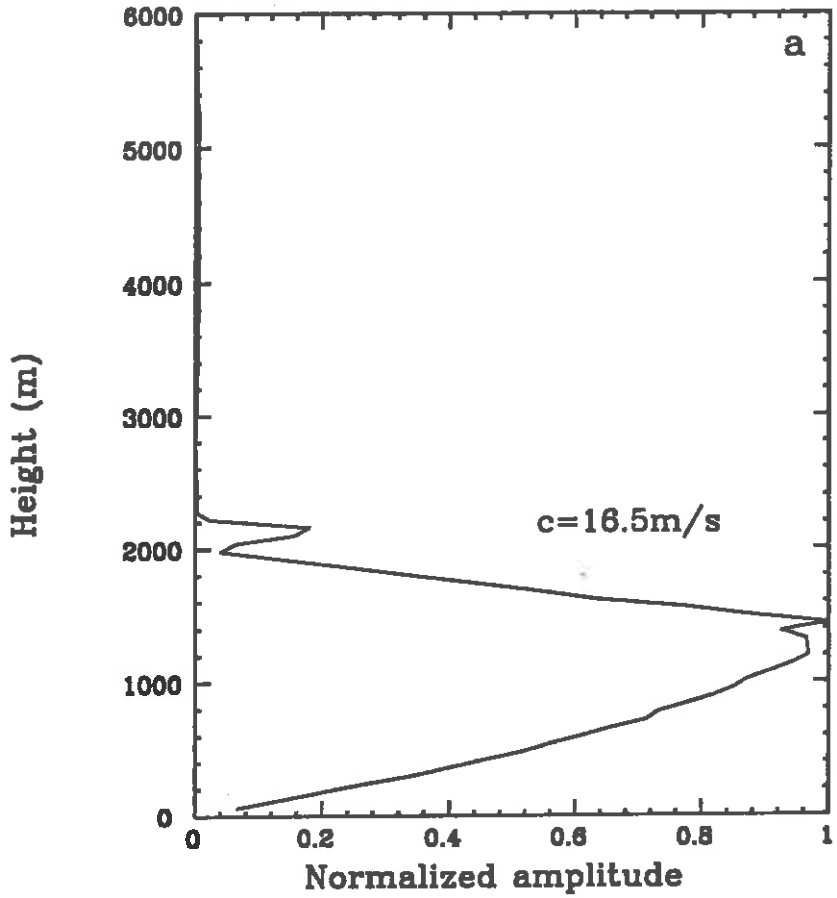
a
c=16.5m/s
Height (m)
Normalized amplitude
6000
5000
4000
3000
2000
1000
0
0
0.2
0.4
0.6
0.8
1

Fig. 9a

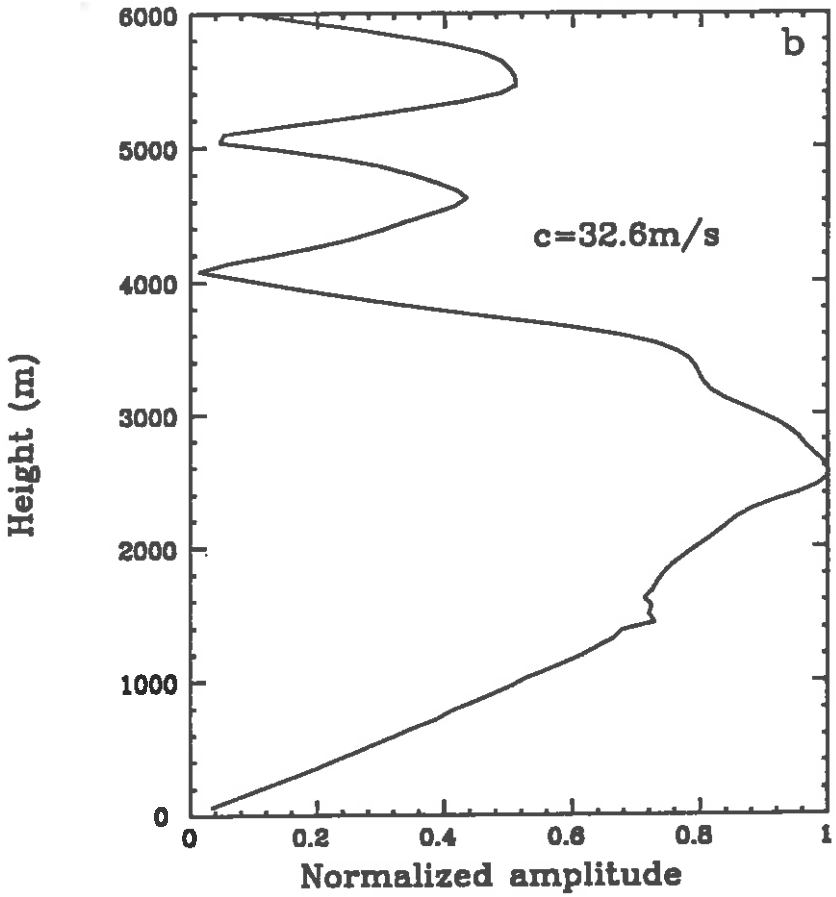
b
c=32.6m/s
Height (m)
Normalized amplitude
6000
5000
4000
3000
2000
1000
0
0
0.2
0.4
0.6
0.8
1

Fig 9.6

CURRENT JCMM INTERNAL REPORTS

This series of JCMM Internal Reports, initiated in 1993, contains unpublished reports and also versions of articles submitted for publication. The complete set of Internal Reports is available from the National Meteorological Library on loan, if required.

1. **Research Strategy and Programme.**
   K A Browning et al
   January 1993

2. **The GEWEX Cloud System Study (GCSS).**
   GEWEX Cloud System Science Team
   January 1993

3. **Evolution of a mesoscale upper tropospheric vorticity maximum and comma cloud from a cloud-free two-dimensional potential vorticity anomaly.**
   K A Browning
   January 1993

4. **The Global Energy and Water Cycle**
   K A Browning
   July 1993

5. **Structure of a midlatitude cyclone before occlusion.**
   K A Browning and N Roberts
   July 1993

6. **Developments in Systems and Tools for Weather Forecasting.**
   K A Browning and G Szejwach
   July 1993

7. **Diagnostic study of a narrow cold frontal rainband and severe winds associated with a stratospheric intrusion.**
   K A Browning and R Reynolds
   August 1993

8. **Survey of perceived priority issues in the parametrizations of cloud-related processes in GCMs.**
   K A Browning
   September 1993

9. **The Effect of Rain on Longwave Radiation.**
   I Dharssi
   September 1993

10. **Cloud Microphysical Processes - A Description of the Parametrization used in the Large Eddy Model.**
    H Swann
    October 1993

11. **An Appreciation of the Meteorological Research of Ernst Kleinschmidt.**
A J Thorpe
May 1992

12. **Potential Vorticity of Flow Along the Alps.**
A J Thorpe, H Volkert and Dietrich Heimann
August 1992

13. **The Representation of Fronts.**
A J Thorpe
January 1993

14. **A Parametrization Scheme for Symmetric Instability: Tests for an Idealised Flow.**
C S Chan and A J Thorpe
February 1993

15. **The Fronts 92 Experiment: a Quicklook Atlas.**
Edited by T D Hewson
November 1993

16. **Frontal wave stability during moist deformation frontogenesis.**
Part 1. Linear wave dynamics.
C H Bishop and A J Thorpe
May 1993

17. **Frontal wave stability during moist deformation frontogenesis.**
Part 2. The suppression of non-linear wave development.
C H Bishop and A J Thorpe
May 1993

18. **Gravity waves in sheared ducts.**
S Monserrat and A J Thorpe
October 1993

Met Office Joint Centre for Mesoscale Meteorology Department of Meteorology
University of Reading PO Box 243 Reading RG6 6BB United Kingdom
Tel: +44 (0)118 931 8425 Fax: +44 (0)118 931 8791
www.metoffice.com